hydrology

MDPI

Article

Mapping Projected Variations of Temperature and Precipitation Due to Climate Change in Venezuela

Jesús A. Viloria [1,*], Barlin O. Olivares [2,*], Pedro García [3], Franklin Paredes-Trejo [4] and Aníbal Rosales [1]

[1] Facultad de Agronomía, Universidad Central de Venezuela, Avenida Universidad Vía El Limón, Maracay 02105, Venezuela
[2] Grupo de Investigación en Gestión de la Biodiversidad, Campus Rabanales, Universidad de Córdoba, Carretera Nacional IV, km 396, 14014 Córdoba, Spain
[3] Grupo Orinoco, Avenida Universidad Vía El Limón, Maracay 02105, Venezuela
[4] Programa de Ciencias Básicas y Aplicada, Departamento de Ingeniería Civil, Universidad Nacional de Los Llanos Ezequiel Zamora, San Carlos 2201, Venezuela
* Correspondence: jesus.viloria@ucv.ve (J.A.V.); ep2olcab@uco.es (B.O.O.)

Abstract: The impacts of climate change will not be homogeneous in all countries or between regions within each country. Mapping projected changes in temperature and precipitation is crucial for formulating region-specific agricultural adaptation measures. The spatial variation of projected changes in temperature and annual precipitation for 1970–2000 and 2041–2060 in Venezuela was analyzed using the WorldClim 2.1 data. Both variables have been analyzed in fourteen physiographic regions that differ in climate, geology, geomorphology, soils, and land use. The results reveal that western regions experience higher temperature increases, while the regions located in the east and center of the country are projected to experience greater decreases in rainfall. Likewise, temperature and precipitation will increase from north to south. Thus, there are differences in how different regions will be affected by variations in temperature and annual precipitation associated with climate change. It is concluded that physiographic regions can be used as large spatial units to plan future land use and design agricultural adaptation measures to climate change at the national scale.

Keywords: agriculture; global climate models; precipitation change; temperature change; water deficit; drought

check for updates

Citation: Viloria, J.A.; Olivares, B.O.; García, P.; Paredes-Trejo, F.; Rosales, A. Mapping Projected Variations of Temperature and Precipitation Due to Climate Change in Venezuela. *Hydrology* **2023**, *10*, 96. https://doi.org/10.3390/hydrology10040096

Academic Editor: Heejun Chang

Received: 17 February 2023
Revised: 14 April 2023
Accepted: 15 April 2023
Published: 17 April 2023

Copyright: © 2023 by the authors. Licensee MDPI, Basel, Switzerland. This article is an open access article distributed under the terms and conditions of the Creative Commons Attribution (CC BY) license (https://creativecommons.org/licenses/by/4.0/).

1. Introduction

Climate change is one of the most pressing global challenges of our time. Some of the principal repercussions of climate change in Venezuela are the rise of the air temperature and the alteration of the country's hydrological cycle, leading to more frequent and intense droughts. Recent studies show that drought is a natural hazard that can cause severe water shortages and can have a significant impact on agriculture [1–4], water resources [5–7], and energy production [8]. Climate change impacts will differ throughout the Venezuelan territory [9–12]. The intensity and temporality of the effects will depend on the current local climate [13,14]. However, information on the geographic distribution of climate change impacts in Venezuela is vague. There is no published information more precise than a reference made to three broad regions (east, center-west, and west) to describe the potential impact of the change in the water regime on agriculture [9]. Knowing the spatial distribution of the changes in temperature and precipitation associated with climate change is crucial to determine the vulnerability of different regions of this country, as well as to identify research needs and formulate geographically specific adaptation measures. Fulfilling this need for information has two requirements. First, to map with greater precision the geographic distribution of the projected impacts of climate change in Venezuela. Second, to associate these impacts to zones with particular physiographic and geographic characteristics, which can be used to design specific adaptation policies for each region.

Mapping the spatial distribution of the potential impacts of climate change in Venezuela is hampered by the lack of reliable climate data, as the available meteorological networks have low spatial coverage, a high proportion of missing data, and records of short duration [15–17]. On the other hand, current computing capabilities have allowed the creation of high-resolution (1 km) climate grids, such as the WorldClim model, over most of the planet. These grids offer new options for climate mapping in data-deficient countries such as Venezuela. They have been used to project climate change impacts on species of agricultural and forestry interest [18–23]. However, there are doubts about the reliability of the information provided by such grids, as spatial climate features supposedly unimportant at a 50 km scale are very important at a 1 km scale. For example, the importance of coastal and relief effects on spatial climate patterns is low at 100 km scales but increases below 10 km. Therefore, areas with significant terrain features and substantial coastal influence are difficult to map accurately [24]. The uncertainty of WorldClim data can be high in mountainous regions and areas with a low density of weather stations due to shortcomings in the interpolation process [25,26]. That is why it is necessary to validate this model before its application. However, many studies lack information on the validity of the WorldClim data used as independent variables [27].

Based on a prior validation of WorldClim 2.1 for Venezuela [27], this study uses data from this model to explore the spatial variation of the changes in annual temperature and annual precipitation between 1970–2000 and 2041–2060. It then compares the results with broad geographic units, called physiographic regions, to see if these can be useful as frameworks for implementing adaptation measures to climate change. The results of this study present an overview of the potential impacts of climate change across the country.

2. Materials and Methods

2.1. Study Area

Venezuela is between 73.4–59.8° W and 0.7–12.2° N in the north of South America (Figure 1a). It has an extension of 916,445 square kilometers, of which approximately 44% corresponds to mountains. Nearly 50% of the Venezuelan territory is under forest, 20% under permanent pastures, 3% under temporary crops, and 1% under permanent crops. Of the total national cultivated area, about 94% is rain-fed and 6% is irrigated. More than 90% of the population lives north of the Orinoco River, where there is most of the country's productive development (Figure 1b). The country has a tropical climate, with a rainier and warmer season from April to September and a cooler and drier season from October to March. The intertropical convergence zone controls the precipitation regime, except in the coastal region affected by tropical disturbances that occur off the coast of northwest Africa. Likewise, subtropical fronts and tropical temperate troughs can favor the occurrence of heavy rains inland at any time of the year [28,29]. Rainfall variability of Venezuelan is a consequence of the country's location in the intertropical zone, north of the equator, with warm waters to the north and northeast (Caribbean Sea and Atlantic Ocean), extensive humid-tropical forests to the south, and large mountain ranges to the west and north [30,31]. In addition, the rainfall regime is also affected by the El Niño-Southern Oscillation (ENSO) phenomenon, whose cold phase (Niña) is associated with humid conditions above average. In comparison, its warm phase (Niño) is related to drier conditions [31,32]. Consequently, precipitation shows a high spatial and temporal variability, while air temperature is a slightly variable factor, characterized by horizontal thermal gradients of small value and vertical gradients described in the climatic literature [27].

2.2. Climatic Data

This research compares climatic data of daily maximum and minimum temperatures, annual maximum and minimum temperatures, annual mean temperature, and average annual precipitation from the late 20th century (1970–2000) to the middle (2041–2060) of the 21st century. These data were obtained from WorldClim 2.1 [23] in raster format (GeoTiff files) with a spatial resolution of 30″ (~1 km^2).

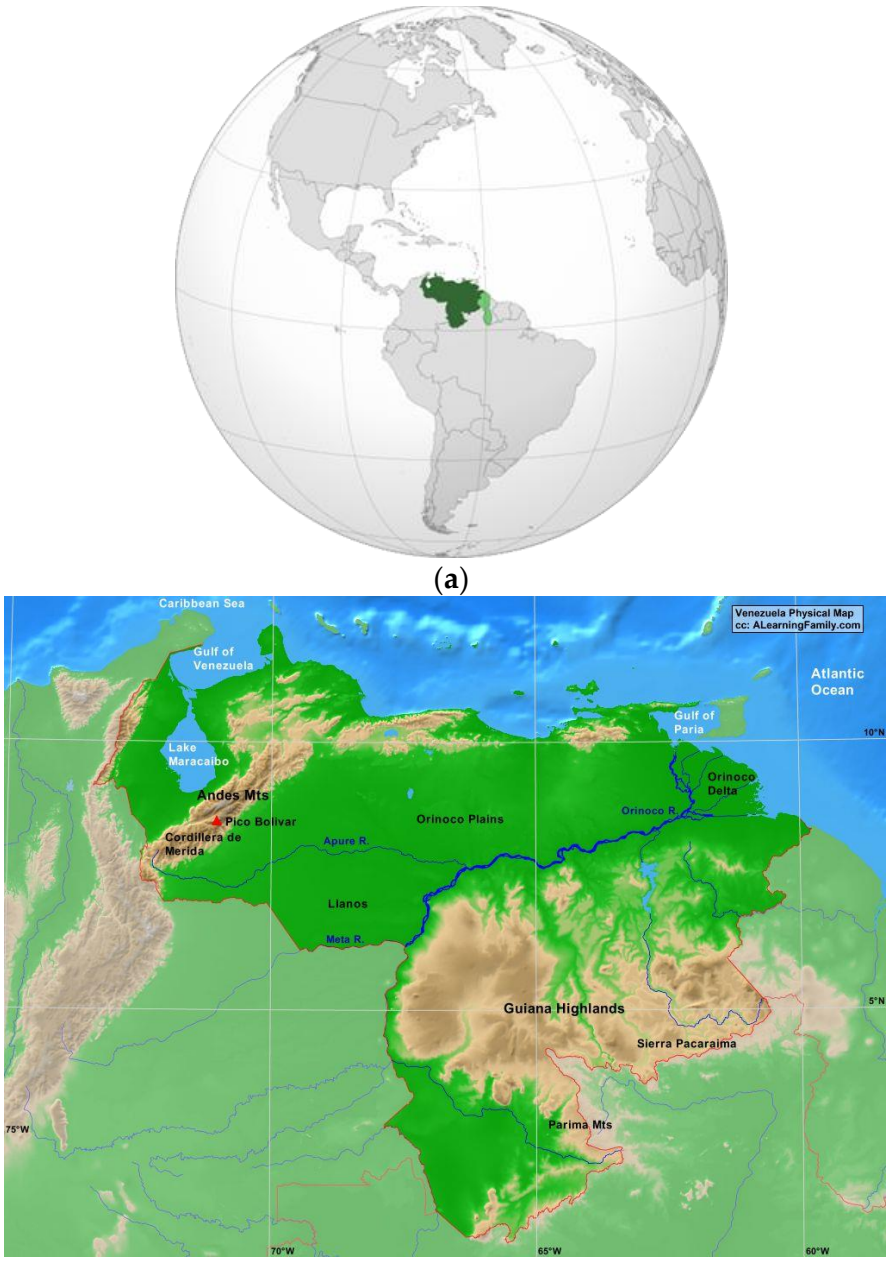


Figure 1. Study area: (**a**) Geographical location, (**b**) Elevation range with brown denoting higher terrain levels. Sources: (**a**) https://ia.wikipedia.org/wiki/Venezuela. (**b**) https://alearningfamily.com/main/venezuela-physical-map. Colors in Figure 1b are as follows: blue = rivers and water bodies; green = 0–500 m above sea level (masl); light brown = 500–1000 masl; medium brown = 1000–2000 masl; dark brown = 2000–5000 masl (accessed on 25 March 2023).

This research used annual precipitation and temperature estimates instead of monthly values, based on a previous evaluation of historical precipitation data generated by WorldClim 2.1. This evaluation statistically compared the WorldClim estimates with data from 185 weather stations and concluded that the monthly precipitation estimates do not reflect Venezuelan conditions. However, the annual precipitation estimates showed a low error rate and high efficiency, so they can be used as independent variables in environmental studies [27].

WorldClim 2.1 includes surfaces of historical data from 1970 to 2000 [33]. These data have been produced by interpolation between weather stations, and adjusted with

information from satellite images and other sources [18]. It also contains future climate data projected by different general circulation models from the CMIP6 (Coupled Model Intercomparison Project Phase 6). Such future data have been grouped into annual averages, for 20-year periods, from 2021 to 2100 [34].

This study used data with a spatial resolution of 30″ (~1 km^2) because this spatial resolution is more appropriate to show the spatial variation of the climatic variables in a country of the dimensions of Venezuela. However, the original data have a coarser resolution that has been transformed by means of a downscaling process. Consequently, the finer resolution does not imply greater realism of the data. The procedure used to downscale the data is explained in [35].

The future data used in this study are climatic projections produced by the general circulation model MPI-ESM1.2-LR (Max Planck Institute Earth System Model) [36] with the SSP3-7.0 scenario. This model is the version of the MPI-ESM model in the Coupled Model Intercomparison Project Phase 6 (CMIP6). The MPI-ESM-LR was one of the four CMIP5 models that showed the best fit for temperature and precipitation in Venezuela [36]. Rainfall and temperature data from this model were utilized to study the oceanic influence on precipitation in Venezuela [37]. In addition, an exploratory evaluation in some locations in Venezuela placed the quality of the estimates of the MPI-ESM-LR in first place among those of nine general circulation models [38].

CMIP conducts periodic comparisons of model climate projections produced by different climate modeling groups around the world. To this aim, it considers alternative scenarios of future emissions and land-use changes. Scenarios included in CMIP6 embody distinct shared socioeconomic trajectories (SSP) and additional radiative forcing due to atmospheric concentrations of greenhouse gases for the 21st century. The SSP3-7.0 scenario supposes a societal development pathway in which policies increasingly focus on national and regional security issues. Nationalism and regional conflicts relegate global matters to the background. Investment in education and technological development decreases and inequality increases. This scenario assumes an additional radiative forcing of 7 W/m^2 by the year 2100 [39,40].

2.3. Regionalization

This study attempts to map the changes in annual temperature and precipitation, between 1970–2000 and 2041–2060, by grids with a spatial resolution of approximately 1 km^2. In addition, it aims to establish whether the spatial variation of these changes can be related to broad geographic units, which could serve as frameworks for planning climate change adaptation strategies. For this purpose, we compared the spatial variation of the predicted changes in these climatic variables with the map of physiographic regions proposed by Elizalde et al. [41] (Figure 2). However, the "Coastal Plains" region was excluded because it consists of a set of small polygons, often smaller than the minimum mappable area with the spatial resolution of this study. Tables A1–A3 briefly describe the physiographic regions used in this study.

2.4. Data Analysis

The study used QGIS 3.22.5 [42] and R Studio 2022.12.0 [43] for data management and analysis. We used the entire population of pixels to compare the projected temperature and precipitation variations between physiographic regions. For this purpose, we applied a spatial analysis procedure known as zonal statistics, which included all the pixels in every region.

In addition, we extracted a random sample of 2100 pixels (150 per region) to determine whether differences between physiographic units were statistically significant at 95% probability. For this purpose, we applied the non-parametric Kruskal–Wallis test [44] because the sampled values did not meet the assumptions of a Gaussian distribution and homogeneity of variances.

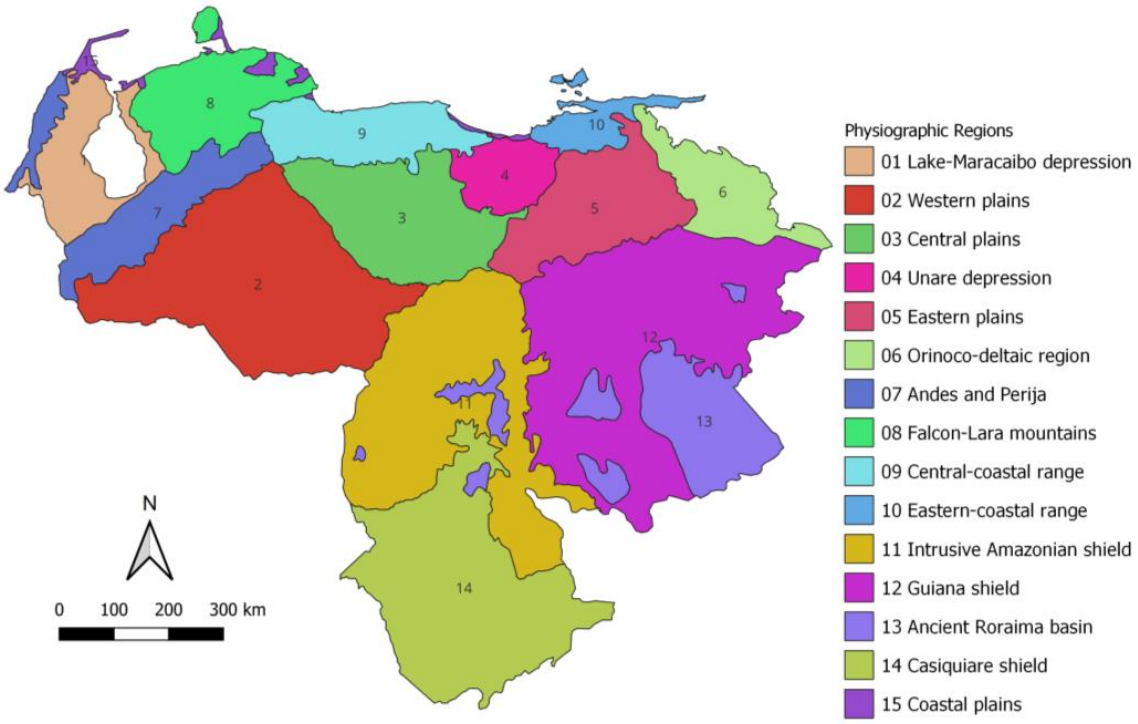


Figure 2. Physiographic regions of Venezuela modified from Elizalde et al. [41].

The Kruskal–Wallis test is a non-parametric hypothesis test that ranks all physiographic regions separately. If the null hypothesis is rejected (not all ranks are significantly different), we perform a post hoc analysis using the Nemenyi pairwise comparison test to identify which physiographic regions differ. The Nemenyi test calculates a mean rank for each physiographic region. If the rank difference between a pair of physiographic regions is greater than or equal to a critical distance (CD), these two regions are significantly different from each other [45,46]. The critical distance is calculated as follows:

$$\mathrm{CD} = q\alpha\sqrt{\frac{k(k+1)}{6n}}$$

where n represents the total number of compared pixels, k represents the number of physiographic regions, and $q\alpha$ is a critical value based on a Studentized range statistic foe $\alpha = 0.05$.

3. Results

3.1. Temperature

Results in Table 1 show that the MPI-ESM1-2-LR model, with the SSP3-7.0 scenario, projects an increase of 0.9 °C on average in annual mean temperature in Venezuela between 1970–2000 and 2041–2060. This temperature increment will vary from 0.1 °C in the Falcón-Lara mountains (region 8) and the Eastern-coastal range (region 10) in the extreme north of the country to 2.4 °C in the Casiquiare shield (region 14) in the extreme south. Figure 3 shows that the mean annual temperature will gradually increase from about 1% in the country's north to 9% in the south, with an intermediate fringe where the temperature will augment 4% to 5% (Figure 3). Consequently, the physiographic regions in the middle and west of the country tend to be internally more heterogenous (Figure 3 and Table 1). However, the variation within these regions is not entirely random; instead, it appears to conform to predictable spatial patterns that can help to divide those regions into more homogeneous units.

Table 1. Projected variation of annual mean temperature (°C) between 1970–2000 and 2041–2060 by physiographic regions.

Physiographic Regions	Number of Pixels	1970–2000	2041–2060	Variation (°C)		Variation (%)	
		°C	°C	Mean	stdv	Mean	stdv
1 Lake-Maracaibo depression	38,110	28.0	28.5	0.5	0.26	1.7	1.0
2 Western plains	148,880	27.2	28.9	1.6	0.38	6.0	1.3
3 Central plains	74,328	27.0	28.2	1.2	0.29	4.4	1.0
4 Unare depression	24,143	26.4	27.2	0.8	0.21	3.0	0.8
5 Eastern plains	63,172	26.7	27.2	0.5	0.35	1.9	1.2
6 Orinoco-deltaic region	36,131	26.4	26.7	0.3	0.18	1.0	0.7
7 Andes and Perija	50,289	20.3	21.0	0.7	0.31	3.4	3.9
8 Falcón-Lara mountains	50,913	25.2	25.4	0.1	0.31	0.5	1.4
9 Central-coastal range	43,244	24.0	24.5	0.4	0.38	1.7	2.0
10 Eastern-coastal range	15,880	23.7	24.1	0.1	0.23	0.5	1.6
11 Intrusive Amazonian shield	137,974	25.7	27.7	2.0	0.45	7.9	2.0
12 Guiana shield	170,477	25.8	26.8	1.1	0.53	4.1	2.2
13 Ancient Roraima basin	69,978	23.4	24.8	1.4	0.39	6.0	1.8
14 Casiquiare shield	131,622	26.2	28.5	2.4	0.24	9.2	1.0
Mean		25.4	26.4	0.9		3.7	

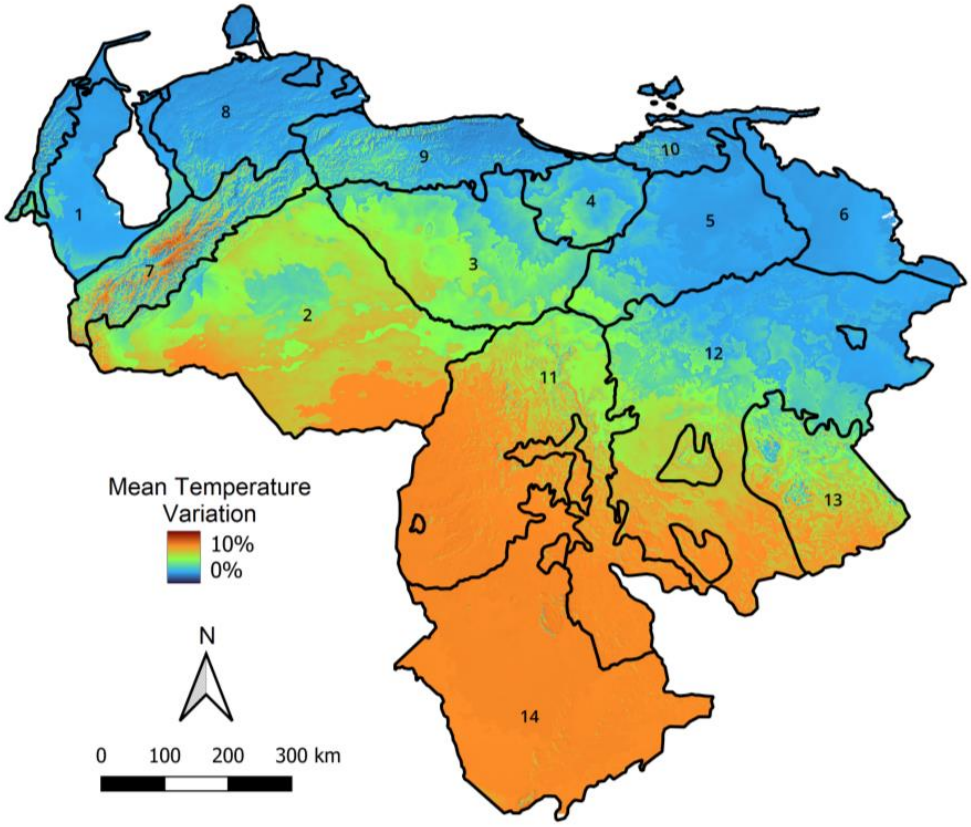


Figure 3. Map of percent of variation of the mean annual temperature between 1970–2000 and 2041–2060 in Venezuela, with the boundaries of the physiographic regions numbered as in Table 1.

In addition to the spatial variation related to latitude and longitude, the projected increment of the mean annual temperature will tend to be higher on the top of the mountain ridges than in the lower lands, as can be seen in Figure 3 (see, for instance, the physiographic unit 7: Andes and Perijá).

The Kruskal–Wallis non-parametric test confirms that, from a statistical point of view, the projected rises in mean annual temperature differ significantly (p = 0.05) between

physiographic regions. Moreover, Table 2 presents the results of the Nemenyi test for comparison between pairs of these regions. This test transformed temperature values into mean ranks and determined a critical distance between them according to the probability level chosen (1.62 at $p = 0.05$). Physiographic regions are significantly different if the disparity between their mean ranks is greater than the critical distance [46]. Based on the results of this test, the physiographic regions can be grouped into five sets (region a to region e). Some physiographic units are transitional between adjacent groups. These results confirm that the projected elevation in mean annual temperature in the southern section of the country (physiographic regions 14, 11, 13, and 12) and the western (region 2) and central plains (region 3) will be significantly greater than in the rest of the country.

Table 2. Mean ranks (MR) computed by the Nemenyi test to the projected increases in annual mean temperature for the different physiographic regions.

Physiographic Regions	MR	MR + CD	Label
1 Lake-Maracaibo depression	2.41	4.03	a
2 Western plains	2.55	4.17	a
3 Central plains	3.17	4.79	ab
4 Unare depression	4.68	6.3	b
5 Eastern plains	4.77	6.39	b
6 Orinoco-deltaic region	6.31	7.93	bc
7 Andes and Perija	7.32	8.94	c
8 Falcón-Lara mountains	7.32	8.94	c
9 Central-coastal range	8.33	9.95	cd
10 Eastern-coastal range	9.43	11.05	d
11 Intrusive Amazonian shield	10.74	12.36	de
12 Guiana shield	11.57	13.19	e
13 Ancient Roraima basin	12.74	14.36	ef
14 Casiquiare shield	13.55	15.17	f

Note: Critical distance (CD) = 1.62, for a significance level of 5%. Differences are statistically significant only between physiographic regions labeled with different letters.

The projected percentage increase in daily minimum and maximum temperature varies between near 0% and 75% (Figures 4 and 5). This range of variation is considerably higher than for the average annual temperature (0.5% to 9%). Changes in minimum and maximum temperatures show different patterns of spatial variation (Figure 4). On the one hand, the minimum daily temperature will increase in the south of the country but will decrease in the north, particularly in some mountainous areas (Figure 4). On the other hand, the projected maximum daily temperature will increase in more than half of the country, including the south, the western plains, the western central plains, the Andes and Perijá, and part of the Cordillera de la central coast (Figure 5).

The projected percentage increase in daily minimum and maximum temperature varies between near 0% and 75%. This range of variation is considerably higher than for the average annual temperature (0.5% to 9%). Changes in minimum and maximum temperatures show different patterns of spatial variation (Figures 4 and 5). On the one hand, the minimum daily temperature will increase in the south of the country but will decrease in the north, particularly in some mountainous areas (Figure 4. On the other hand, the projected maximum daily temperature will increase in more than half of the country, including the south, the western plains, the western central plains, the Andes and Perijá, and part of the Cordillera de la central coast (Figure 5).

3.2. Precipitation

According to the MPI-ESM1-2-LR model with the SSP3-7.0 scenario, the annual mean precipitation in Venezuela will decrease by 100 mm on average between 1970–2000 and 2041–2060 (Table 3). The rainfall reduction will vary across the country from around 200 mm in the physiographic regions 6 (Orinoco-deltaic region), 12 (Guiana shield), and

13 (Ancient Roraima basin) to less than zero in the physiographic unit 14 (Casiquiare shield), where the model projects a slight increment of 14 mm.

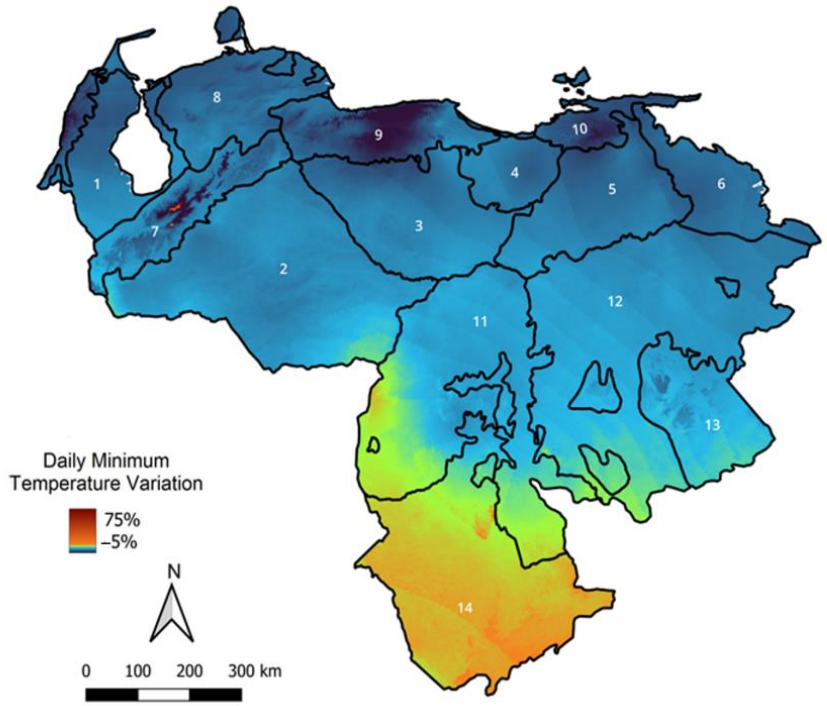


Figure 4. Maps of projected changes in daily minimum temperature between 1970–2000 and 2041–2060 in Venezuela, with the boundaries of the physiographic regions numbered as in Table 3.

Table 3. Projected variation of annual precipitation by physiographic region between 1970–2000 and 2041–2060.

Physiographic Regions	Number of Pixels	1970–2000	2041–2060	Variation mm		Variation %	
		mm	mm	Mean	stdv	Mean	stdv
1 Lake-Maracaibo depression	38,612	1429	1398	−31	18.1	−3	1.6
2 Western plains	148,959	1790	1758	−32	77.5	−2	4.1
3 Central plains	74,328	1278	1157	−121	23.3	−10	1.8
4 Unare depression	24,143	1070	961	−109	42.5	−10	1.9
5 Eastern plains	63,172	1174	1045	−129	54.3	−11	2.7
6 Orinoco-deltaic region	36,652	1705	1511	−194	70.5	−12	3.6
7 Andes and Perija	50,554	1357	1294	−63	27.4	−5	2.1
8 Falcón-Lara mountains	51,209	845	784	−61	19.1	−7	2.4
9 Central-coastal range	43,665	1137	1027	−110	20.7	−10	1.1
10 Eastern-coastal range	17,439	1141	1078	−63	76.6	−5	3.8
11 Intrusive Amazonian shield	140,028	2435	2359	−76	67.2	−3	2.5
12 Guiana shield	172,857	2021	1828	−193	76.5	−10	2.8
13 Ancient Roraima basin	70,482	2307	2076	−231	100.1	−10	3.2
14 Casiquiare shield	134,848	2956	2970	14	61.5	0	2.0
Mean		1618	1518	−100		−3	

Figure 6 and Table 3 reveal that the annual rainfall will decline by around 10% in most of the east and north of the country, while in the west and south, it will drop by 2% to 6%. The figure also shows that the physiographic regions reasonably describe the spatial variation in the projected changes in annual mean precipitation. Moreover, the Kruskal–Wallis non-parametric test verifies that the projected precipitation decline differs significantly (p = 0.05) between physiographic regions. However, as the spatial variation is gradual, the rainfall reduction changes between and within regions. Thus,

the internal differences in rainfall shrinkage between pixels in the same physiographic unit range from 8% to 20%, but Figure 6 shows spatial trends that can help model this within-region variation.

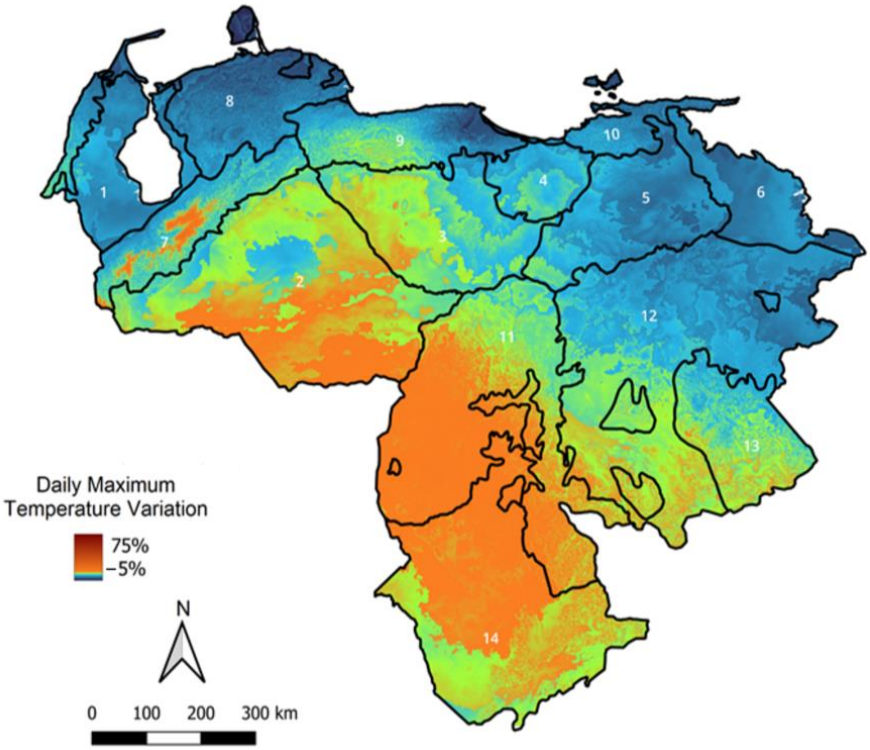


Figure 5. Maps of projected changes in daily maximum temperature between 1970–2000 and 2041–2060 in Venezuela, with the boundaries of the physiographic regions numbered as in Table 3.

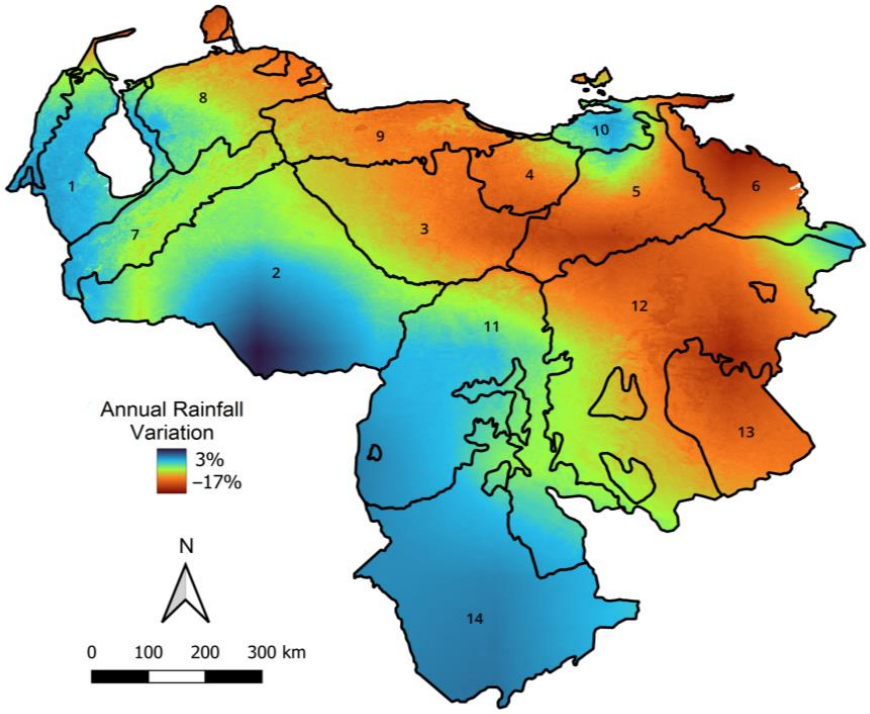


Figure 6. Map of projected changes in annual mean precipitation (mm) between 1970–2000 and 2041–2060 in Venezuela, with the boundaries of the physiographic regions numbered as in Table 4.

Table 4. Mean ranks (MR) computed by the Nemenyi test to the projected decreases in annual mean precipitation for the different physiographic regions.

Physiographic Regions	MR	MR + CD	Label
1 Lake-Maracaibo depression	2.93	4.55	a
2 Western plains	3.21	4.83	a
3 Central plains	3.49	5.11	a
4 Unare depression	5.43	7.05	b
5 Eastern plains	5.77	7.39	b
6 Orinoco-deltaic region	6.14	7.76	b
7 Andes and Perija	6.56	8.18	b
8 Falcón-Lara mountains	8.63	10.25	c
9 Central-coastal range	8.71	10.33	c
10 Eastern-coastal range	9.54	11.16	cd
11 Intrusive Amazonian shield	9.76	11.38	cd
12 Guiana shield	10.7	12.32	de
13 Ancient Roraima basin	11.87	13.49	ef
14 Casiquiare shield	12.46	14.08	f

Note: Critical distance (CD) for a significance level of 5%. = 1.62. Differences are statistically significant only between physiographic regions labeled with different letters.

The results of the Nemenyi test (Table 4) reveal the existence of five groups of physiographic regions significantly different from each other ($p = 0.05$), concerning the projected reduction in precipitation. The first group includes regions 13 (Ancient Roraima basin), 6 (Orinoco-deltaic region), and 12 (Guiana shield), which will suffer the most considerable reduction in precipitation. The second group includes regions 5 (Eastern plains), 3 (Central plains), 9 (Central-coastal range), and 4 (Unare depression), which will experience an intermediate reduction. Finally, the third group includes all other physiographic regions in which the decrease in precipitation will be smaller.

4. Discussion

This study models the spatial variation of the projected changes in annual temperature and annual precipitation between 1970–2000 and 2041–2060 in Venezuela as continuous surfaces of one square kilometer cells. Such models show that the projected changes in precipitation and temperature will vary throughout the Venezuelan territory, which confirms observations by other authors [1,6,7,9–11] regarding the spatial variation of climate change impacts in this country. According to the MPI-ESM1-2-LR model projections with the SSP3-7.0 scenario, between 1970–2000 and 2041–2060, the mean annual temperature will increase by a relatively small proportion (about 1%) in northern Venezuela. This increase will grow progressively in a north–south and east–west direction to reach about 9%. The projected increase in mean annual temperature will also tend to be greater at the top of the mountain ranges than in the lowlands. The temperature increase will be more uniform in the north and south physiographic units than in the central and western regions. Among the latter, the central plains (region 3), the western plains (region 2), and the Andes (region 7) stand out for their agricultural importance. The mean annual precipitation will decrease by 10% to 12% (100 to 200 mm per year) in the east and north of Venezuela and 3% or less in the south, west, and northwest. According to the model, there could be a slight increase in average annual precipitation in the Casiquiare shield (region 14) in the extreme south. The spatial variability of the projected annual precipitation changes will be greater in some regions than others. Among the regions with considerable internal variability, it is worth mentioning the eastern plains (region 5), the central plains (region 3), the western plains (region 2), and the Andes (region 7). A large part of the country's agricultural production occurs in these regions.

The study's results reveal that there are spatial relationships between the projected changes in precipitation and temperature throughout the country and the physiographic regions proposed by Elizalde et al. [41]. These regions delimit areas based on solid com-

ponents of the landscape (rocks, regolith, sediments, and soils) that are less variable in time and space than climate, biota, and the results of human activities [41]. Therefore, such regions are potentially stable frameworks for decision-making on climate change adaptation measures at a national level tailored to geographic specificities. However, the continuous surfaces of cells show some variation in the projected precipitation and temperature changes within the physiographic regions. Consequently, the physiographic regions will require further division for designing climate change adaptation measures at more detailed geographic levels. The within-region variation shows spatial patterns that can help to model it for such a purpose.

The increase in temperature in Venezuela could cause damage to biodiversity and agricultural production, as well as hurt human health, due to an increase in heat-related diseases [47,48]. Likewise, rising temperatures can increase heat waves' frequency and severity, leading to crop loss or reduced yields [49–51]. The impact of temperature change in the western and central plains on crops, cattle, and field workers is a matter of concern for the agricultural importance of these regions. In extensive areas of these plains, the projected values for daily maximum temperature (34 °C) are higher than the critical limits for some common species cultivated in Venezuela, such as maize (*Zea mays* L.), the common bean (*Phaseolus vulgaris* L.), and cocoa (*Theobroma cacao* L.) [50].

On the other hand, the alteration of the country's hydrological cycle could have a significant impact on agriculture, as well as on water resources and energy production [8,46]. In addition, changes in rainfall patterns can also lead to increased pest and disease pressure, damaging crops and reducing yields [51]. Our results project that the mean annual rainfall will decrease by more than 100 mm in the physiographic regions Orinoco-deltaic region, Eastern plains, Unare depression, and the east of the central plains. These results coincide with the findings reported on meteorological droughts in agricultural territories of the central plains [52–54]. This precipitation reduction will probably be associated with a higher risk of sequences of dry days during the rainy season, which is already a limitation for rain-fed crops in these regions.

Thus, in the north half of the country, the eastern plains will experience more precipitation decreases but less temperature increases than the western plains. Moreover, the Lake Maracaibo depression, in the country's northwest, will also be affected by temperature increases and precipitation decreases, but with fewer changes than the other plains. Consequently, each region needs different specific measures to adapt to climate change.

The increment in annual mean temperature in the Andes and Central coast ranges will be greater than in the Eastern-coastal range and the Falcón-Lara mountains. Daily minimum and maximum temperature changes will be similar in the different mountain ranges north of the Orinoco River. Likewise, a greater decrease in annual precipitation is projected in the Central-coastal range than in the other mountain ranges. However, it should be kept in mind that the uncertainty in precipitation data in WorldClim is larger in mountainous areas due to spatial variability and imperfections in the interpolation [18,55].

In the southern part of the country, the intrusive Amazonian shield and the Casiquiare shield will experience higher temperature increases than in the rest of the country. Likewise, the precipitation in the Guiana Shield and the Ancient Roraima basin will decrease to a greater extent than in the rest of the country. The area potentially affected by this decrease in precipitation covers an extensive sector of the Caroní River basin, which could impact the endemic species of this region and trigger forest fires. It could also seriously impact the water inflow to the Bajo (Lower) Caroní hydroelectric reservoirs, including the Guri one, which supplies about 70% of the national electricity demand [56,57].

The projected temperature and precipitation changes will likely modify agroclimatic conditions and land-use suitability in some of the regions analyzed [58–60]. This, in turn, will lead to transformations in Venezuela's agricultural production systems and in the use of rural spaces. Climate change may also have important economic and social implications. The impacts on agriculture could increase food insecurity, the loss of biodiversity could affect the tourism industry, and the increase in temperature could generate higher energy

consumption [61]. Venezuela's vulnerability to climate change impacts is high. The country has a high level of poverty and part of its population is engaged in agriculture and fisheries [62], which are sectors particularly vulnerable to climate change impacts [63–65]. For these reasons, it is important to consider projected variations in temperature and precipitation due to climate change when making decisions about economic and social development and environmental protection in Venezuela.

This study's findings have significant academic, scientific, and technical potential, as they provide valuable information that can be used to inform decision-making around climate change adaptation and mitigation in Venezuela. Here, it is necessary to insist on the exploratory nature of these results given the uncertainty of the data, especially in mountainous and near-coastal areas. Further research is needed to understand the full implications of the study, as well as to identify potential solutions and strategies for managing climate change in the country. The novelty and originality of this research lie in its comprehensive approach to the issue, which provides a detailed overview of the expected temperature and precipitation changes across the country. Additionally, the results of the research have the potential to have a major impact on the lives of Venezuelans, as the findings can inform strategies for adapting to and mitigating the impacts of climate change.

5. Conclusions

Geospatial data analysis made it possible to represent the spatial variation of the changes in annual precipitation and temperature projected for 2041–2060, as continuous surfaces of one square kilometer cells. This analysis also revealed spatial relationships between a vectorial model of physiographic regions and the projected changes in annual temperature and precipitation throughout the country. These regions delimit potentially useful areas as stable frameworks for national decision-making on geographically specific climate change adaptation measures.

The temperature increases in the western lowlands (Western plains and west of the Central plains) will be higher than in the eastern lowlands (Orinoco-deltaic region, Eastern plains, Unare depression, and east of the Central plains). In contrast, the eastern lowlands will suffer a greater reduction in precipitation than the western lowlands. On the other hand, the Lake Maracaibo depression will suffer a minor increase in temperature and a smaller decrease in precipitation than the other plains located north of the Orinoco River.

Among the mountain ranges north of the Orinoco River, the Andes will experience the most significant increases in annual minimum and maximum temperatures. In contrast, the Central-coastal range will suffer the most significant decreases in total annual rainfall. In addition, the increase in annual mean temperature in the Andes and the Central-coastal range will be higher than in the Eastern-coastal range and the Falcón-Lara mountains. Nationwide, the intrusive Amazonian shield and the Casiquiare shield will experience the highest temperature increases, while the Guiana shield and the Ancient Roraima basin will experience the largest precipitation decreases.

The described differences between the physiographic regions corroborate that each region needs different specific measures to adapt to climate change. However, this study's results are subject to uncertainties in the input data, especially in mountainous and near-coastal areas. Therefore, they are working hypotheses that should be tested locally.

Climate change is expected to have significant impacts on biodiversity and water resources in the south of the state of Bolivar and Amazonas in Venezuela. One potential impact of climate change on biodiversity is the loss of habitat. As temperatures increase, many species may be forced to migrate to find suitable habitat, while others may not be able to adapt to the changing conditions and may face extinction. This could have ripple effects throughout the ecosystem, disrupting food webs and altering the composition of species in the region.

Overall, Venezuela is particularly vulnerable to changes in temperature and precipitation patterns associated with climate change. However, it is essential to ensure that the factors responsible for environmental changes in different regions are accurately identi-

fied to implement the appropriate interventions. Therefore, it is crucial to conduct more in-depth regional scientific studies to determine whether climate change is the sole cause of environmental changes or if other factors are contributing. Conducting detailed studies can provide valuable insights into the specific causes of environmental changes, enabling policymakers and stakeholders to implement targeted interventions that address the root causes of the problem. Ultimately, regional scientific studies are essential for developing comprehensive strategies to combat climate change and ensure the sustainable use of natural resources.

Author Contributions: Conceptualization, J.A.V., A.R. and P.G.; methodology, J.A.V.; software, J.A.V.; validation, J.A.V., F.P.-T., A.R., P.G. and B.O.O.; formal analysis, J.A.V.; investigation, J.A.V., B.O.O. and F.P.-T.; resources, B.O.O., F.P.-T., A.R. and P.G.; data curation, J.A.V.; writing—original draft preparation, J.A.V., B.O.O., F.P.-T., A.R. and P.G.; writing—review and editing, J.A.V., B.O.O., F.P.-T., A.R. and P.G. visualization, J.A.V.; supervision, B.O.O., F.P.-T., A.R. and P.G. All authors have read and agreed to the published version of the manuscript.

Funding: This research received no external funding.

Data Availability Statement: Not applicable.

Conflicts of Interest: The authors declare no conflict of interest.

Appendix A

Table A1. Physiographic regions of the plains north of the Orinoco River according to Elizalde et al. [43].

Physiographic Regions	Description
Lake Maracaibo depression	It is a tectonic subsidence filled by sedimentary rocks and Quaternary sediments with altitudes ranging from 0 to 500 m above sea level (masl). The predominant relief configurations are the Maracaibo plateau and alluvial plains. Precipitation increases from <500 mm/yr in the north to 3550 mm/yr in the southwest. The distribution of the vegetation responds to the precipitation pattern. The variability of climate, relief, parent materials, and age determine a wide diversity of soils.
Western plains	These flat and low areas encompass different combinations of fluvial plains and some eolian plains of the Holocene and Upper Pleistocene. The dominant elevation is 100 masl but can vary between 500 and <50 masl. Drainage routes flow south–southeast or eastward. Part of the region is well-drained. Drainage is poor towards the center and southeast of the region, with frequent flooding. Precipitation rises from east to west and from north to south. Vertical and horizontal variability of soils is significant.
Central plains	They correspond to undulating erosion plains of low hills with gently sloping convex tops, separated by very open inter-collinear depressions. The difference in elevation between the tops and the bases of the hills ranges between 50 and 80 m. The average altitude of the region is <250 masl. The predominant rocks are sedimentary, aged between the Upper Cenozoic and Pleistocene. Stony, shallow, acidic soils predominate in the hills, while deep, fine, acidic soils predominate in the valleys. In the south, there is an area of sandy dunes alternating with poorly drained depressions.
Eastern plains	They have a topography of low mesa, with flat or undulating tops and heights less than 350 masl, formed on horizontal sedimentary layers of the Mesa Formation (Pleistocene). Boxed valleys of variable width and less than 50 m depth are between the mesas. Well-drained sandy soils dominate the mesas with increasing clay content at depth and low moisture retention, as well as being acidic with deficient nutrient and organic matter content. In the valleys, the soils are more fertile and have high spatial variability, with poor drainage in some areas.
Unare depression	It resulted from the erosion of Tertiary clayey sedimentary rocks alternating with sandstones. The topography consists of hills, with denudation surfaces and accumulations of sediments from the slopes between the hills. The average altitude is about 150 masl. The soils are predominantly deep, well-drained, clayey, and cracked when dry.

Table A1. *Cont.*

Physiographic Regions	Description
Orinoco-deltaic region	It includes the Orinoco Delta and the plain of the San Juan River in the country's extreme east. The topography is flat and low (<15 masl). Drainage is poor, conditioned by topography, rainfall, the rivers that cross the region, and the Atlantic Ocean and the Caribbean Sea tides. On the surface, there are recent mineral sediments rich in clay, silt, and organic matter, alternating with organic sediments (peat) that are not very decomposed. The predominant vegetation is mangroves, and swamps in the areas are influenced by the tides, while forests and grasslands dominate where fresh water accumulates. The soil is recent and rich in organic matter, and those affected by tides contain iron sulfide (pyrite).

Table A2. Physiographic regions of the mountain range north of the Orinoco River according to Elizalde et al. [43].

Physiographic Regions	Description
Andes and Perijá	Its predominant configuration comprises medium and high mountains and deep valleys, with narrow or wide bottoms filled with sediments arranged in terraces. The average altitudes are 2000 to 3000 masl, with maximum altitudes close to 5000 masl. It presents a folded geological structure. The central core consists of metamorphic rocks (gneisses and schists) and granites of the Precambrian and Paleozoic; the flanks are composed of Tertiary rocks. Annual precipitation varies from less than 400 mm to more than 2000 mm, and annual mean temperature varies from $\pm 0^{\circ}$ C at the highest peaks to $\pm 24^{\circ}$ C at the lowest sites in the region. Due to the variability of the factors described above, there is a great diversity of soils.
Falcón-Lara mountains	These are low and medium mountains, with narrow V-shaped or wide intra- and inter-mountain valleys filled with alluvial and colluvial sediments arranged in terraces. The average heights of the mountains vary between 1000 and 1500 masl and the valley bottoms are between 600 and 900 masl. The oldest rocks in the region are metamorphic and belong to the Mesozoic, but those that cover more extension are Cenozoic rocks with folded, fractured structures, and incipient metamorphism.
Central-coastal range	They are mountain ranges of medium and low altitudes, separated by intra- and inter-mountain V-shaped valleys with narrow bottoms and valleys with wide bottoms filled with sediments often arranged in terraces. In addition, it contains tectonic depressions filled with sediments, such as the Lake Valencia depression and Barlovento. It extends approximately 300 km east–west and 100 km north–south. The average altitude is between 1000 and 1200 masl and the maximum altitude is higher than 2700 masl. There are Paleozoic rocks in the region, but the most extensive and representative units consist of Mesozoic metamorphic rocks. There is a wide diversity of soil products from variations in climate, vegetation, relief, parent materials, and time of evolution.
Eastern-coastal range	It corresponds to the mountainous and hilly reliefs found in the northeastern portion of the country, made up of low- and medium-altitude mountain ranges, intra- and inter-montane V-shaped valleys with narrow bottoms and tectonic depressions filled with sediments. It extends for about 300 km in an east–west direction and approximately 100 km in a north–south direction. The average altitudes range between 1200 and 1400 masl above sea level and the maximum altitudes reach 2500 to 2600 masl. Metamorphic and sedimentary rocks from the Mesozoic are predominant, and, as in the other mountainous areas, there is a wide diversity of soils.

Table A3. Physiographic regions south of the Orinoco River according to Elizalde et al. [43].

Physiographic Regions	Description
Intrusive Amazonian shield	Its physiography is variable, including mountains, plateaus, and erosion plains. Acid intrusive rocks of Precambrian age (>2000 million years old), such as granite and granodiorite, are predominant. The dominant vegetation covers are evergreen forests and wooded savannas. Soils are strongly acidic with poor fertility.
Guiana shield	It consists of peneplains formed by hills and hillocks, whose predominant rocks are gneisses and granites of the Precambrian age. The vegetation cover varies from wooded savannas and deciduous forests to evergreen forests. Prevalent are strongly weathered soils that are acidic, poorly fertile, and well-drained.

Table A3. *Cont.*

Physiographic Regions	Description
Ancient Roraima basin	It comprises various discontinuous highlands, including the "Gran Sabana", and some elevated plateaus or tepuis of a tabular and practically horizontal structure formed by sedimentary rocks of the Roraima Group. They are remnants of an ancient Precambrian basin. Predominant soils have low humidity retention and scarce nutrient availability.
Casiquiare shield	It is south of the 4th parallel. It consists predominantly of plains and peneplains of erosion or alteration derived from Precambrian migmatites, gneisses, and granites. The soils are strongly weathered, acidic, and poorly fertile.

References

1. Márquez, Y.P.; Moreno, E.C. Potential distribution of crops in Mérida State (Venezuela), under climatic change scenarios. *Rev. Geográfica Venez.* **2021**, *62*, 428–444. [CrossRef]
2. Jaimez, R.; Loor, R.; Arteaga, F.; Márquez, V.; Tezara, W. Differential response of photosynthetic activity, leaf nutrient content and yield to long-term drought in cacao clones. *Acta Agronómica* **2022**, *70*, 274–284. [CrossRef]
3. Olivares, B.; Cortez, A.; Parra, R.; Lobo, D.; Rodríguez, M.F.; Rey, J.C. Evaluation of agricultural vulnerability to drought weather in different locations of Venezuela. *Rev. Fac. Agron.* **2017**, *34*, 103–129. Available online: https://n9.cl/d827w (accessed on 25 March 2023).
4. Olivares, B.; Zingaretti, M.L. Analysis of the meteorological drought in four agricultural locations of Venezuela by the combination of multivariate methods. *UNED Res. J.* **2018**, *10*, 181–192. [CrossRef]
5. Paredes-Trejo, F.; Barbosa-Alves, H.; Moreno-Pizani, M.A.; Farías-Ramírez, A. Influencia de las sequías sobre el régimen hídrico de los ríos en Venezuela. *Ríos Riesgo Venez.* **2018**, *2*, 171–184. Available online: https://n9.cl/3xs3d (accessed on 25 March 2023).
6. Chacón-Moreno, E.; Rodríguez-Morales, M.; Paredes, D.; Suárez del Moral, P.; Albarrán, A. Impacts of Global Change on the Spatial Dynamics of Treeline in Venezuelan Andes. *Front. Ecol. Evol* **2021**, *9*, 615223. [CrossRef]
7. Silva, M.I.; Mendoza, N. Assessment of meteorological drought in agricultural locations from Venezuela under future projections of climate change. *Rev. Fac. Agron.* **2021**, *38*, 548–572. [CrossRef]
8. Paredes-Trejo, F.; Olivares, B. El desafío de la sequía en Venezuela. In *Atlas de Sequía de América Latina y el Caribe*; Núñez, C.J., Verbist, K., Eds.; UNESCO: Paris, Francia, 2018; pp. 127–136. Available online: https://n9.cl/h3ay4 (accessed on 25 March 2023).
9. Ovalles, F.; Cabrera, E.; Cortéz, A.; Rodríguez, M.F.; Rey, J.C. *Formulación de Lineamientos Generales Para un Programa de Adaptación a Los Posibles Impactos de Los Cambios Climáticos Sobre el Sector Agrícola en Venezuela, Considerando Tres Escenarios (2015, 2040 y 2060)*; Proyecto MARN–PNUD VEN/00/G31. INIA: Maracay, Venezuela, 2005.
10. Martelo, M.T. Impact of climate change on agriculture in Venezuela. *Rev. Fac. Agron. UCV* **2012**, *71*, 66–81.
11. Medina, E.; Velásquez, G.; Hernández, I. Impact of global warming and atmospherico CO_2 enrichment on tropical crops: A perspective for Venezuela. *Rev. Fac. Agron. UCV* **2016**, *42*, 25–37.
12. Olivares, B.; Hernández, R.; Coelho, R.; Molina, J.C.; Pereira, Y. Spatial analysis of the water index: Advances in sustainable decision-making in Carabobo agricultural territories, Venezuela. *Rev. Geográfica América Cent.* **2018**, *60*, 277–299. [CrossRef]
13. Zhang, Y.; Fu, B.; Feng, X.; Pan, N. Response of ecohydrological variables to meteorological drought under climate change. *Remote Sens.* **2022**, *14*, 1920. [CrossRef]
14. IPCC. Climate Change 2022: Impacts, Adaptation, and Vulnerability. Contribution of Working Group II. In *Sixth Assessment Report of the Intergovernmental Panel on Climate Change*; Pörtner, H.-O., Roberts, D.C., Tignor, M., Poloczanska, E., Mintenbeck, K., Alegría, A., Craig, M., Langsdorf, S., Löschke, S., Möller, V., et al., Eds.; Cambridge University Press: Cambridge, UK, 2022; *in press*.
15. Guenni, L.; Degryze, E.; Alvarado, K. Análisis de la tendencia y la estacionalidad de la precipitación mensual en Venezuela. *CoJS* **2008**, *31*, 41–65.
16. Vila, D.A.; de Goncalves, L.; Toll, D.L.; Rozante, J.R. Statistical evaluation of combined daily gauge observations and rainfall satellite estimates over continental South America. *J. Hydrometeorol.* **2009**, *10*, 533–543. [CrossRef]
17. Olivares, B.; Parra, R.; Cortez, A. Characterization of precipitation patterns in Anzoátegui state, Venezuela. *Ería* **2017**, *3*, 353–365. [CrossRef]
18. Fick, S.E.; Hijmans, R.J. Worldclim 2: New 1-km spatial resolution climate surfaces for global land areas. *Int. J. Clim.* **2017**, *37*, 4302–4315. [CrossRef]
19. Dutta, R. Climate change and its impact on tea in Northeast India. *J. Water Clim. Chang.* **2014**, *5*, 625–632. [CrossRef]
20. Bunn, C.; Läderach, P.; Pérez Jimenez, J.G.; Montagnon, C.; Schilling, T. Multiclass Classification of Agro-Ecological Zones for Arabica Coffee: An Improved Understanding of the Impacts of Climate Change. *PLoS ONE* **2015**, *10*, e0140490. [CrossRef]
21. Läderach, P.; Ramirez–Villegas, J.; Navarro-Racines, C.; Zelaya, C.; Martinez–Valle, A.; Jarvis, A. Climate change adaptation of coffee production in space and time. *Clim. Chang.* **2017**, *141*, 47–62. [CrossRef]

22. Babalik, A.A.; Sarikaya, O.; Orucu, O.K. The Current and future compliance areas of Kermes Oak (Quercus coccifera L.) under climate change in Turkey. *Fresenius Environ. Bull.* **2021**, *30*, 406–413. Available online: https://hdl.handle.net/20.500.12885/1407 (accessed on 17 February 2023).
23. Sondermann, M.; Chou, S.C.; Lyra, A.; Latinovic, D.; Siqueira, G.C.; Junior, W.C.; Giornes, E.; Leite, F.P. Climate change projections and impacts on the eucalyptus plantation around the Doce River basin, in Minas Gerais, Brazil. *Clim. Serv.* **2022**, *28*, 100327. [CrossRef]
24. Daly, C. Guidelines for assessing the suitability of spatial climate data sets. *Int. J. Climatol.* **2006**, *26*, 707–721. [CrossRef]
25. Zheng, P.; Fang, P.; Liu, P.; Xu, W.; Wang, G.; Wang, L. Dominate Tree Species Classification on Large-Scale Mountainous Areas Using Voting Strategy-Based Ensemble Learning Method. In *Proceedings of the 8th China High Resolution Earth Observation Conference (CHREOC 2022)*; Springer: Singapore, 2023; pp. 102–115.
26. Karger, D.N.; Wilson, A.M.; Mahony, C.; Zimmermann, N.E.; Jetz, W. Global daily 1 km land surface precipitation based on cloud cover-informed downscaling. *Sci. Data* **2021**, *8*, 307. [CrossRef]
27. Fernández, G.; Milla, D. Validez de los datos de precipitación media mensual (1970–2000) generados por el modelo WorldClim V2. 0 para Venezuela. *Terra. Nueva Etapa* **2018**, *34*. Available online: https://n9.cl/axbqn (accessed on 17 February 2023).
28. Paredes, F.J.; Alves Barbosa, H.; Peñaloza-Murillo, M.A.; Moreno, M.A.; Farias, A. Intercomparison of improved satellite rainfall estimation with CHIRPS gridded product and rain gauge data over Venezuela. *Atmósfera* **2016**, *29*, 323–342. [CrossRef]
29. Olivares, B.; Hernández, R. Regional analysis of homogeneous precipitation zones in Carabobo, Venezuela. *Rev. Lasallista Investig* **2019**, *16*, 90–105. [CrossRef]
30. Olivares, B. Tropical conditions of seasonal rain in the dry-land agriculture of Carabobo, Venezuela. *La Granja Rev. Cienc. Vida* **2018**, *27*, 86–102. [CrossRef]
31. Cortez, A.; Rodríguez, M.F.; Rey, J.C.; Ovalles, F.; González, W.; Parra, R.; Olivares, B.; Marquina, J. Temporary space variability of precipitation in Guarico state, Venezuela. *Rev. Fac. Agron.* **2016**, *33*, 292–310. Available online: https://n9.cl/pmdck (accessed on 17 February 2023).
32. Veettil, B.K.; Wang, S.; de Souza, S.F.; Bremer, U.F.; Simoes, J.C. Glacier monitoring and glacier-climate interactions in the tropical Andes: A review. *J. S. Am. Earth Sci.* **2017**, *77*, 218–246. [CrossRef]
33. WorldClim Historical Climate Data. Available online: https://www.worldclim.org/data/worldclim21.html (accessed on 22 September 2022).
34. WorldClim Future Climate, 30 Seconds Spatial Resolution. Available online: https://www.worldclim.org/data/cmip6/cmip6_clim30s.html (accessed on 23 September 2022).
35. WorldClim Downscaling Future and Past Climate Data from GCMs. Available online: https://www.worldclim.org/data/downscaling.html (accessed on 15 March 2023).
36. Gutjahr, O.; Putrasahan, D.; Lohmann, K.; Jungclaus, J.H.; von Storch, J.-S.; Brüggemann, N.; Haak, H.; Stössel, A. Max Planck Institute Earth System Model (MPI-ESM1.2) for the High-Resolution Model Intercomparison Project (HighResMIP). *Geosci. Model Dev.* **2019**, *12*, 3241–3281. [CrossRef]
37. Gómez, J.A.; Pérez, G.J.M. Evaluación de los modelos climáticos del IPCC AR5 para Venezuela. In *Primer Reporte Académico de Cambio Climático de Venezuela (PRACC)*; Academia de Ciencias Físicas, Matemáticas y Naturales de Venezuela, Villamizar, A., Buroz Castillo, E., Lairet Centeno, R., Gómez, J.A., Eds.; Ediciones ACFIMAN–CITECI: Caracas, Venezuela, 2018.
38. Tim, N.; Bravo de Guenni, L. Oceanic influence on the precipitation in Venezuela under current and future climate. *Clim. Dyn.* **2016**, *47*, 211–234. [CrossRef]
39. Silva, O.; Universidad Central de Venezuela, Aragua, Venezuela. Personal Communication, 2022.
40. O'Neill, B.C.; Tebaldi, C.; van Vuuren, D.P.; Eyring, V.; Friedlingstein, P.; Hurtt, G.; Knutti, R.; Kriegler, E.; Lamarque, J.F.; Lowe, J.; et al. The Scenario Model Intercomparison Project (ScenarioMIP) for CMIP6. *Geosci. Model Dev.* **2016**, *9*, 3461–3482. [CrossRef]
41. Elizalde, G.; Viloria, J.A.; Rosales, A. Geografía de Suelos de Venezuela. In *Geo Venezuela, Tomo 2: Medio Físico y Recursos Ambientales*; Fundación Empresas Polar: Caracas, Venezuela, 2007; pp. 402–537.
42. QGIS.org. QGIS Geographic Information System. QGIS Association. Available online: http://www.qgis.org (accessed on 17 February 2023).
43. R Core Team. *R: A Language and Environment for Statistical Computing*; R Foundation for Statistical Computing: Vienna, Austria; Available online: https://www.R-project.org/ (accessed on 17 February 2023).
44. Kruskal, W.H.; Wallis, W.A. Use of ranks in one-criterion variance analysis. *J. Am. Stat. Assoc.* **1952**, *47*, 583–621. [CrossRef]
45. Nemenyi, P. Distribution-Free Multiple Comparisons. Ph.D. Thesis, Princeton University, Princeton, NJ, USA, 1963.
46. Liu, Y.; Chen, W. A SAS macro for testing differences among three or more independent groups using Kruskal-Wallis and Nemenyi tests. *J. Huazhong Univ. Sci. Technol. Med. Sci. J.* **2012**, *32*, 130–134. [CrossRef]
47. Beyrer, C.; Page, K. Preventable losses: Infant mortality increases in Venezuela. *Lancet Glob. Health* **2019**, *7*, e286–e287. [CrossRef]
48. Page, K.R.; Doocy, S.; Ganteaume, F.R.; Castro, J.S.; Spiegel, P.; Beyrer, C. Venezuela's public health crisis: A regional emergency. *Lancet* **2019**, *393*, 1254–1260. [CrossRef]
49. Bonacic, C.; Arévalo, C.; Ibarra, J.T.; Laker, J. The Importance of Protected Areas in Mitigating Climate Change and Conserving Ecosystems in Latin America and the Caribbean. In *The Food Security, Biodiversity, and Climate Nexus*; Springer: Cham, Switzerland, 2022; pp. 35–53.

50. Teixeira, A.; Da Silva, D.A.; Gonçalves, J.G.R.; Esteves, J.A.F.; Carbonell, S.A.M.; Chiorato, A.F. Root characterization of bean genotypes (*Phaseolus vulgaris*) under drought stress. *Genet. Mol. Res.* **2019**, *18*, GMR18086. [CrossRef]
51. Ruiz, C.J.A.; Medina, G.; González, I.J.; Flores, H.E.; Ramírez, G.; Ortiz, C.; Byerly, K.F.; Martínez, R.A. Requerimientos agroecológicos de cultivos. In *Libro Técnico Núm. 3*, 2nd ed.; INIFAP. Instituto Nacional de Investigaciones Forestales Agrícolas y Pecuarias-CIRPAC-Campo Experimental Centro Altos de Jalisco: Tepatitlán de Morelos, México, 2013; 564p.
52. Cortez, A.; Olivares, B.; Parra, R.; Lobo, D.; Rodríguez, M.F.; Rey, J.C. Event description of meteorological drought in locations central mountains, Venezuela. *Cienc. Ing. Appl.* **2018**, *I*, 22–44.
53. Cortez, A.; Olivares, B.; Parra, M.; Lobo, D.; Rey, J.C.; Rodriguez, M.F. Systematization of the calculation of the Standardized Precipitation Index as a methodology to generate meteorological drought information. *Rev. Fac. Agron.* **2019**, *36*, 209–223. Available online: https://n9.cl/4spjp (accessed on 17 February 2023).
54. Olivares, B.; Zingaretti, M.L. Application of multivariate methods for the characterization of periods of meteorological drought in Venezuela. *Luna Azul* **2019**, *48*, 172–192. [CrossRef]
55. Marchi, M.; Sinjur, I.; Bozzano, M.; Westergren, M. Evaluating WorldClim Version 1 (1961–1990) as the Baseline for Sustainable Use of Forest and Environmental Resources in a Changing Climate. *Sustainability* **2019**, *11*, 3043. [CrossRef]
56. Bautista, S.A. sustainable scenario for Venezuelan power generation sector in 2050 and its costs. *Energ. Policy* **2012**, *44*, 331–340. [CrossRef]
57. Moreno-Pizani, M.A. Water management in agricultural production, the economy, and Venezuelan society. *Front. Sustain. Food Syst.* **2021**, *4*, 624066. [CrossRef]
58. Tapia, M.S.; Puche, M.; Pieters, A.; Marrero, J.F.; Clavijo, S.; Gutiérrez, S.; Machado-Allison, C.; Raffalli, S.; Herrera, M.; de Jiménez, M.L.; et al. Seguridad alimentaria y nutricional en Venezuela. Secuestro Agroalimentario de un País: Visión y Compromiso. In *Retos y oportunidades de la seguridad alimentaria en las Américas. El punto de vista de las Academias de Ciencias*; Clegg, M., Bianchi, E., McNeil, J., Estrella, L.H., Vammen, K., Eds.; La Red Interamericana de Academias de Ciencias (IANAS); Red Mundial de Academias de Ciencias (IAP); El Ministerio Federal de Educación e Investigación Bundesministerium für Bildung und Forschung (BMBF); Academia Nacional de Ciencias de Alemania: Leopoldina, México, 2017; Available online: http://www.ianas.org (accessed on 30 September 2020).
59. Olivares, B.; Hernández, R.; Arias, A.; Molina, J.C.; Pereira, Y. Agroclimatic zoning of corn crop for sustainable agricultural production in Carabobo, Venezuela. *Rev. Univ. Geog.* **2018**, *27*, 139–159. Available online: https://n9.cl/l2m83 (accessed on 17 February 2023).
60. Santana, P.A., Jr.; Kumar, L.; Da Silva, R.S.; Pereira, J.L.; Picanço, M.C. Assessing the impact of climate change on the worldwide distribution of Dalbulus maidis (DeLong) using MaxEnt. *Pest Manag. Sci.* **2019**, *75*, 2706–2715. [CrossRef]
61. Paredes-Trejo, F.J.; Barbosa-Alves, H.; Moreno-Pizani, M.A.; Farías-Ramírez, A. Cambio climático: Altera el régimen de precipitaciones y caudales en Venezuela? In *Ríos en Riesgo de Venezuela Vol. 3*; Rodríguez-Olarte, D., Ed.; Universidad Centroccidental Lisandro Alvarado: Barquisimeto, Venezuela, 2020; pp. 37–147.
62. Trejo, F.J.P.; Barbosa, H.A.; Ruiz, I.Q.; Peñaloza-Murillo, M.A. Meso scale oceanic atmospheric circulation patterns linked with severe and extensive droughts in Venezuela. *Rev. Bras. Meteorol* **2016**, *31*, 468–489. [CrossRef]
63. Olivares, B.; Hernández, R. Application of multivariate techniques in the agricultural land's aptitude in Carabobo, Venezuela. *Trop. Subtrop. Agroecosyst.* **2020**, *23*, 1–12. Available online: https://n9.cl/zeedh (accessed on 17 February 2023).
64. Paredes, F.; Millano, J.L.; Guevara, E. Spatial analysis of meteorological droughts in the Los Llanos region of Venezuela during the period 1961–1996. *Rev. Climatol.* **2008**, *8*, 15–27.
65. Paredes, F.; La Cruz, F.; Guevara, E. Regional frequency analysis of meteorological droughts in the largest cereals producing region of Venezuela. *Bioagro* **2014**, *26*, 21–28.

Disclaimer/Publisher's Note: The statements, opinions and data contained in all publications are solely those of the individual author(s) and contributor(s) and not of MDPI and/or the editor(s). MDPI and/or the editor(s) disclaim responsibility for any injury to people or property resulting from any ideas, methods, instructions or products referred to in the content.